Cytochrome P450 BM3 as versatile biocatalytic tool in drug development

Rea, V.

2012

document version
Publisher's PDF, also known as Version of record

CHAPTER 2

ROLE OF RESIDUE 87 IN SUBSTRATE- AND REGIOSELECTIVITY OF DRUG METABOLIZING CYTOCHROME P450 BM3 M11

Eduardo Vottero, Vanina Rea, Jeroen Lastdrager, Maarten Honing, Nico P.E. Vermeulen and Jan N.M. Commandeur

---

adapted from *Journal of Biological Inorganic Chemistry,* 2011, 16(6), 899-912

Abstract:

BM3, originating from *Bacillus megaterium,* is a highly active enzyme which has attracted much attention because of its potential applicability as a biocatalyst for oxidative reactions. Previously we developed a drug metabolizing mutant BM3 M11 by a combination of site-directed and random mutagenesis. BM3 M11 contains ten mutations, when compared to wild-type BM3 and is able to produce human-relevant metabolites of several pharmaceuticals. In this study, active-site residue 87 of drug metabolizing mutant BM3 M11 was mutated to all possible natural amino acids in order to investigate its role in substrate selectivity and regioselectivity. With alkoxyresorufins as substrates, large differences in substrate-selectivities and coupling efficiencies were found, dependent on the nature of residue 87. For all combinations of alkoxyresorufins and mutants extremely fast rates of NADPH-oxidation were observed (up to 6000 min^{-1}). However, the coupling efficiencies were extremely low: even for the substrates showing highest rates of *O*-dealkylation, coupling efficiencies were lower than 1%. With testosterone as substrate, all mutants were able to produce three hydroxytestosterone metabolites although at different activities and with remarkably different product ratios. The results show that the nature of amino acid at position 87 has a strong effect on activity and regioselectivity in the drug-metabolizing mutant BM3 M11. Because of the wide substrate selectivity of BM3 M11 when compared to wild-type BM3, this panel of mutants will be useful both as biocatalysts for metabolite production and as model proteins for mechanistic studies on the function of P450s in general.

2.1. Introduction

Cytochrome P450 BM3 (BM3; EC 1.14.14.1) from *Bacillus megaterium* is a soluble protein that catalyzes the hydroxylation and epoxidation of several long-chain fatty acids. BM3 contains a heme and reductase domain fused in a single polypeptide, which might explain why this enzyme has the highest activity ever reported for a P450 (*1, 2*). By using site-directed and/or random mutagenesis, several research groups have succeeded in broadening the substrate selectivity of this enzyme with the objective to create highly efficient biocatalysts to be used for several biotechnological applications (*3-5*).

In parallel, many mechanistic studies have been devoted to rationalize the roles of various active site residues in substrate selectivity and in the catalytic cycle (*1*). One of the most studied active-site residues is Phe87, which is in close proximity to the heme according to the crystal structures of BM3 (*1*).

In the substrate-free crystal, this residue lies perpendicular to the heme at the end of the substrate access channel. Upon binding of substrate, the orientation of Phe87 changes to parallel to the plane of the heme, thereby influencing the orientation of the substrate relative to the catalytic centre (*6*). Many studies have been performed in which Phe87 of wild-type BM3 or mutants of BM3 has been mutated to other amino acids, as summarized in Table 1. Typically, in these studies one to maximally four different mutations at position 87 were compared. In most cases Phe87, was mutated to amino acids with small non-polar side chains (Gly, Ala, Leu, Ile, Val), whereas only two uncharged polar amino acids (Ser, Tyr) were evaluated. Dependent on the substrate tested and the enzyme template, the type of mutation of Phe87 has differential effects on catalytic properties of P450 (Table 1), which are rationalized by the changes in active site volume, thereby restricting or improving access to the reactive oxygen species at the heme-center (*7-21*).

In this study, all 20 natural amino acids were evaluated at position 87 of BM3 M11. Twelve of the possible amino acids substitutions have not been described previously in wild-type or mutants of BM3. The mutants were characterized using a homologous series of alkoxyresorufins and testosterone as substrates. Alkoxyresorufines are sensitive and useful probes to determine substrate selectivity of both bacterial and mammalian P450 isoforms by the continuous fluorimetric assay of resorufin formed by *O*-dealkylation (*23-25*). Testosterone and other steroids have been shown to be hydroxylated by BM3 mutants (*26, 27*). Testosterone is an excellent probe substrate to study the effect of position 87 on regioselectivity because it can be hydroxylated at multiple positions dependent on the nature of P450-isoenzymes (*28*). Furthermore, there is a great interest in biocatalysts capable to stereo- and regioselectively hydroxylate steroids, because steroid compounds rank among the most widely marketed products from pharmaceutical industry (*29*). We therefore studied whether regioselectivity of steroid hydroxylation by BM3 can be manipulated by mutations at position 87.

Table 1. Effect of mutation of residue 87 on regio-/stereoselectivity of wild-type and mutant BM3

Mutation	Template	Substrate	Effect	Ref.
F87G	wild type	lauric acid	less active; biphasic kinetics; changed regioselectivity	9, 19
	wild type	propylbenzene, chlorostyrene	more active; changed regio-/stereoselectivity	11
F87A	wild type	lauric acid, palmitic acid	less active; changed regioselectivity	7, 18, 19
	wild type	farnesol	more active; changed regioselectivity	18
	wild type	fluoranthene, phenanthrene, pyrene	more active; changed regioselectivity	10
	wild type	propylbenzene	changed regioselectivity	11
	wild type	chlorostyrene	less active; higher enantioselectivity	11
	wild type	(+)-valencene	changed regioselectivity	21
	wild type	resveratrol	less active	20
	A328I	(+)-valencene	more active	21
	A328F	limonene	more active	21
	R47L/Y51F	(+)-valencene	changed regioselectivity	14
	R47L/Y51F	resveratrol	less active	20
	9-10A	phenyl acetic acid esters, buspirone	more active; higher enantioselectivity	16
	C(73-78)	lauric acid, palmitic acid, farnesol	less active	18
	C(75-80)	lauric acid, palmitic acid, farnesol	less active; unchanged regioselectivity	18
	C(78-82)	lauric acid, palmitic acid, farnesol	less active	18

Table 1 (continued)

F87V	wild type	lauric acid	less active; changed regioselectivity	19
	wild type	arachidonic acid, eicopentenoic acid	less active; changed regioselectivity	8
	wild type	aromatic and phenolic compound	more active; changed regioselectivity	15
	wild type, A328L	geranyl acetone	more active; changed regioselectivity	21
	A328I, A328V	(+)-valencene	more active; changed regioselectivity	21
	R47L; R47L/L188Q	benzyl- and pentoxyresorufin	more active	13
F87L	wild type	lauric acid	less active; changed regioselectivity	18
	wild type	geranyl acetone	less active; changed regioselectivity	21
	A328I	(+)-valancene	more active	21
	A328V	limonene, geranyl acetone	less active	21
	C(73-78); C(75-80)	lauric acid, palmitic acid, farnesol	less active	18
	C(78-82)	lauric acid, palmitic acid	less active	18
	C(78-82)	farnesol	more active; changed regioselectivity	18
F87I	wild type	geranyl acetone	more active; changed regioselectivity	21
	A328I	(+)-valancene	more active	21
	A328V	limonene, geranyl acetone	less active	21
F87S	wild type	lauric acid	changed regioselectivity	19
F87Y	wild type	lauric acid	lower NADPH-consumption; biphasic kinetics	9
	wild type	N-palmitoyl glycine	inactive; 100% uncoupled	17
	wild type	arachidonic acid, eicopentenoic acid	inactive; 100% uncoupled	8

2.2. Materials and Methods

2.2.1. Materials

All chemicals were of analytical grade and obtained from standard suppliers. Alkoxyresorufins (methoxy- to *n*-octyloxyresorufin) and benzyloxyresorufin were synthesized as described previously (*24*). The pET28a+ vector containing wild-type BM3 was kindly provided by dr. V. Urlacher (Institut für Technische Biochemie, Universität Stuttgart, Germany).

2.2.2 Library construction

Site-directed mutants of BM3 M11 at position 87 were constructed by mutagenic PCR using the Stratagene QuikChange XL site–directed mutagenesis kit (Stratagene, La Jolla, CA, USA) using 20 complementary pairs of mutagenesis primers. The mutagenic PCR was applied to a pBluescript vector (pBS P450 BM3 M11) containing the gene of the drug metabolizing BM3 M11, flanked by *Eco*RI and *Bam*HI restriction sites. BM3 M11 contains mutations R47L, E64G, F81I, F87V, E143G, L188Q, Y198C, E267V, H285Y and G415S when compared to wild-type BM3 (*10*). The sequence of the forward primers was as follows: 5'-GCA GGA GAC GGG TTA **XXX** ACT AGT TGG ACG CAT-3'. **XXX** represents the codon that was used to introduce the specific mutation at position 87. The reverse primer for the mutagenic PCR was a 34-mer 5'-CAT GCG TCC AAC TAG T**YY** **Y**TA ACC CGT CTC CTG C-3' in which **YYY** is the reverse complement of codon **XXX**. The underlined bases indicate a new *Spe*I digestion site. The following codons (**XXX**) were used: Ala, GCC; Arg, CGG; Asn, AAC; Asp, GAC: Cys, UGC; Gln, CAG; Glu, GAG; Gly, GGG; His, CAC; Ile, AUC; Leu, CUG, Lys, AAG; Met, AUG; Phe, UUC; Pro, CCC, Ser, UCC; Thr, ACC; Trp, UGG; Tyr, UAC, and Val, GUG. After mutagenic PCR, the plasmids were digested with *Eco*RI and *Bam*HI restriction enzymes and the genes of mutated BM3 M11 were cloned into a pET28a+ vector, which encodes for a N-terminal His-tag. The desired mutations in the P450 domain were confirmed by DNA sequencing (Baseclear, Leiden, The Netherlands).

2.2.3 Expression and purification of the mutants

Expression of the BM3 mutants and wild-type BM3 was performed by transforming competent *Escherichia coli* BL21 cells with the corresponding pET28+-vectors, as described previously (*21*). Proteins were purified using nickel nitroacetic acid agarose, after which P450 concentrations were determined according to Omura and Sato (*30*). The purity of the enzymes was checked by SDS-PAGE electrophoresis on 12% gel and subsequent Coomassie-staining.

2.2.4 Metabolism of alkoxyresorufins by BM3-mutants

The enzyme activities of the mutants and wild-type BM3 toward a homologues series of alkoxyresorufins were measured according to Burke et al. (*23*) with modifications. To determine *O*-dealkylation activities, fluorescence cuvettes (1.5 mL volume) were filled

with 860 µL of 100 mM potassium phosphate buffer (pH 7.4), 20 µL of 1 µM BM3 (20 nM final concentration) and 20 µL of 1 mM alkoxyresorufine in DMSO (final concentrations: 20 µM alkoxyresorufin, 2% DMSO). After 30 seconds of preincubation, reactions were started by addition of 100 µL of a mixture of 2 mM NADPH, 3 mM glucose-6-phosphate and 0.4 units/mL glucose-6-phosphate dehydrogenase. The increase in fluorescence was monitored at an excitation wavelength of 532 nm and an emission wavelength of 586 nm for 2 minutes at 25°C. Specific activities were determined in triplicate by measuring the initial slopes of resorufin formation. The Shimadzu RF-1501 spectrofluorimeter used was calibrated by addition of 10 µL of 1 µM resorufine to the cuvet, and by recording the increase in fluorescence (*23*). The results are means of duplicate determinations, with duplicates typically differing by less than 5% from the mean.

To investigate the involvement of hydroxylation of *n*-alkoxy-substituents at other carbons, 10 µL samples of incubations were analyzed by an Agilent 2000 UPLC-system using a Zorbax Eclipse XDB-C18 column (1.8 µm, 50 x 4.6 mm; Agilent, USA). Samples were eluted at a flow rate of 2 mL/min using a gradient composed of solvent A (99.8% water, 0.2% formic acid) and solvent B (99.8% acetonitrile, 0.2% formic acid). The gradient was programmed as follows: from 0 to 1 minutes isocratic 40% B; 1 to 8 minutes linear increase from 40% to 100% B; from 8 to 8.5 minutes isocratic 100% B; from 8.5 to 9 minutes, linear decrease from 100% to 40% B; from 9 to 10 minutes isocratic 40% B. Alkoxyresorufines were detected at 460 nm. Under these conditions the following retention times were obtained: methoxyresorufin, 2.84 min; ethoxyresorufin, 3.57 min; *n*-propyloxyresorufin, 4.20 min; *n*-butoxyresorufin, 5.27 min; *n*-pentoxyresorufin, 6.06 min; *n*-hexoxyresorufin, 6.82 min; *n*-heptoxyresorufin, 7.55 min; *n*-octoxyresorufin, 8.21 min.

2.2.5. Metabolism of testosterone by BM3 mutants

Incubations of BM3 mutants (200 nM) with testosterone (0.5 mM) as substrate were performed at 25 ^{o}C in a total volume of 250 µL in 100 mM potassium phosphate buffer (pH 7.4). Reactions were started by adding 25 µL of a mixture of 2 mM NADPH, 3 mM glucose-6-phosphate and 4 units/mL glucose-6-phosphate dehydrogenase (final concentrations: 0.2 mM NADPH, 0.3 mM glucose-6-phosphate and 0.4 units/mL glucose-6-phosphate dehydrogenase), and were terminated after 60 minutes by addition of 250 µL of cold methanol. Samples were centrifuged for 15 minutes at 4000 rpm, after which supernatants were transferred to HPLC vials.

Testosterone and metabolites were analyzed by high-resolution UPLC (*31*) using an Agilent 2000-system using a Zorbax Eclipse XDB-C18 column (1.8 µm, 50 x 4.6 mm; Agilent, USA). Metabolites and substrate were eluted at a flow-rate of 1.3 mL/min using a gradient composed of solvent A (99.8% water, 0.2% formic acid) and solvent B (99.8% methanol, 0.2% formic acid) The gradient was programmed as follows: from 0 to 2 minutes linear increase from 60% to 100% B; from 2 to 3 minutes isocratic 100% B; from 3 to 3.2 minutes

linear decrease from 100% to 60% B; from 3.2 to 5 minutes isocratic 60% B. Metabolites and substrate were detected at 254 nm.

2.2.6. NADPH-Consumption

NADPH-consumption was quantified spectroscopically by monitoring the decrease in absorbance at 340 nm using an extinction coefficient of 6210 $M^{-1}cm^{-1}$. Cuvettes (1.5 mL volume; 1 cm path length) were filled with 880 µL of 100 mM potassium phosphate buffer (pH 7.4) and 20 µL of 1 µM BM3 mutant (final concentration 20 nM). Reactions were performed at 25 ^{o}C and started by addition of 100 µL of 2 mM NADPH (final concentration 200 µM), after which the decrease of NADPH was monitored for 2 minutes. To determine substrate-induced NADPH-consumption, cuvettes were filled with 860 µL of 100 mM potassium phosphate buffer (pH 7.4), 20 µL of 1 mM of alkoxyresorufin (dissolved in DMSO) and 20 µL of 1 µM BM3 mutant. Reactions were started by addition of 100 µL of 2 mM NADPH, after which the decrease of NADPH was monitored for 2 minutes. To correct for the solvent DMSO, incubations were also performed by adding 20 µL DMSO.

The coupling efficiencies of the BM3 mutants which were able to metabolize alkoxyresorufins were calculated from the ratio of the initial rate of product formation and the initial rate of NADPH consumption.

To investigate whether NADPH consumption is induced by binding to the substrate binding site, incubations were also performed in presence of 1 µM ketoconazole, which was shown to be a very potent inhibitor of BM3 mutants, including BM3 M11 (*13, 32*). To test whether wild-type BM3 can also be inhibited by ketoconazole, inhibition of NADPH consumption induced by 100 µM lauric acid was studied.

2.2.7. UV-vis Spectroscopy

For a selection of the BM3 mutants, the type of substrate binding and spectral dissociation constants (K_D) were determined for four substituted resorufins (methoxyresorufin, *n*-butyloxyresorufin, *n*-heptoxyresorufin and benzyloxyresorufin) using UV-vis difference spectroscopy. UV-vis spectra were recorded at room temperature using a Shimadzu UV-2501PC spectrophotometer (Shimadzu Duisburg, Germany).

All substrate-induced binding spectra were recorded using tandem cuvettes (10 mm path length) to eliminate absorbance by alkoxyresorufins.

Briefly, 1 mL of 2 µM enzyme in 100 mM potassium phosphate buffer (pH 7.4) was added to one of the chambers of the sample and reference tandem cuvette. The other chambers were filled with an equal volume of 100 mM potassium phosphate buffer. The enzyme-containing chamber of the sample cuvette was titrated with microliter volumes of ethanol solutions of alkoxyresorufins, resulting in final concentrations ranging from 1 to 30 µM. In the reference cuvette, the same volume of alkoxyresorufin-solutions was added to the chamber containing buffer only. To correct for effects of ethanol, equal volumes of

ethanol were added to the chambers without alkoxyresorufin. At each concentration of substrate a UV-vis difference spectrum was recorded from 500 to 350 nm.
The observed differences in absorption between 390 nm (peak) and 419 nm (trough), $\Delta A_{390-419}$, were plotted versus alkoxyresorufin concentration after correction for dilution and were analyzed by nonlinear regression, using GraphPad Prism 4 (GraphPad Sotware Inc., San Diego, CA, USA). The spectral binding constants (K_D) were determined by fitting the titration binding curves using to the following equation:

$$\Delta A_{390-419} = \frac{\Delta A_{\infty} * [S]^n}{K_D^n + [S]^n}$$

Where ΔA_{∞} represents the maximal difference at saturating alkoxyresorufin concentration, K_D is the dissociation constant of the enzyme-substrate complex and n is the Hill coefficient.

2.3. Results

2.3.1. Expression and characterization of the BM3 M11-mutants.

Transformation of *E.coli* BL21 with the pET28+-vectors encoding the different BM3 M11-mutants and subsequent purification resulted in significantly different yields of BM3 mutants, ranging from 27 to 666 nmol P450 per liter of original growth medium (Table 2). After purification by nickel nitriloacetic acid agarose, protein purity was always higher than 98% according to SDS-PAGE. For four of the purified mutants containing Pro87, Asp87, Glu87 and Ser87, the reduced CO difference spectra only showed a peak at 420 nm. Formation of P420 is considered to result from coordination of a neutral thiol (in case of BM3 Cys400) to the heme-iron, instead of a thiolate which is required to produce the active P450 (*33*).
Mutation F87S, when applied to wild-type BM3 was previously shown to be an active enzyme with changed regioselectivity in lauric acid hydroxylation (*19*). However, carbon-monoxide difference spectroscopy only showed P420, suggesting that Ser87 is denaturing owing to sodium dithionite treatment [V. Urlacher, personal communication]. Because the concentration of these mutants could not be quantified they were not further evaluated in our metabolism experiments.
The mutant containing Asn87 showed a significant peak at 420 nm with intensity of almost equal to that at 450 nm. Mutants containing Met87, His87 and Gly87 showed a small shoulder at 420 nm next to the peak at 450 nm. All other mutants only produced peaks with maxima ranging from 448 and 450 nm.

Table 2: Spectroscopic properties and yield of the BM3 M11-mutants

#	Residue	Reduced-CO difference spectra: Max (nm)	Reduced-CO difference spectra: A_{450} /A_{420} ratio	P450 Yield (nmoles/L of growth media)
Non-polar side chain:				
1.	Phe87	450	> 100	165
2.	Gly87	423, 449	78	148
3.	Ala87	449	> 100	51
4.	Leu87	449	> 100	237
5.	Ile87	449	> 100	581
6.	Val87 [a)]	449	> 100	666
7.	Met87	423, 448	12.1	344
8.	Pro87	420	n.d.	n.q.
9.	Trp87	450	> 100	27
Uncharged polar side chain:				
10.	Ser87	422	n.d.	n.q.
11.	Thr87	449	> 100	203
12.	Asn87	421, 450	1.2	132
13.	Gln87	448	> 100	49
14.	Tyr87	448	> 100	585
15.	Cys87	450	> 100	41
Charged polar side chain:				
16.	Lys87	448	> 100	91
17.	Arg87	449	> 100	173
18.	His87	423, 450	5.8	80
19.	Asp87	420	n.d.	n.q.
20.	Glu87	420	n.d.	n.q.

a) Val87, BM3 M11, containing R47L, E64G, F81I, F87V, E143G, L188Q, Y198C, E267V, H285Y and G415S.
n.d.: not detectable peak at 450 nm.
n.q.: not quantifiable due to absence of peak at 450 nm.

2.3.2. Alkoxyresorufin metabolism by the BM3 M11-mutants.

2.3.2.1. O-dealkylation activities

Table 3 shows that the specific activities of *O*-dealkylation of nine different alkoxyresorufins measured in incubations with sixteen variants of BM3 M11 were very strongly affected by the nature of the amino acid at position 87. On average, the highest *O*-dealkylation activities were observed with mutants containing non-polar side chains Ala87, Gly87 and Val87. Of the polar residues, Tyr87 was most active, showing significant activity with all alkoxyresorufins, except with methoxyresorufine as substrate. The mutants containing the charged residues only showed low activities to all alkoxyresorufins. Under the present conditions, Lys87, Met87 and Trp87 did not show significant *O*-dealkylation activity with any alkoxyresorufin.

When comparing *O*-dealkylation activity between the different *n*-alkoxy-substituted substrates (methoxyresorufin to *n*-octoxyresorufin), we found that the compounds with shortest *n*-alkoxy-substituent were poorly metabolized. Methoxyresorufin was not *O*-demethylated by any of the mutants, whereas for ethoxyresorufin and *n*-propyloxyresorufine only two and three mutants, respectively, showed activity. The longer the *n*-alkoxy-group, the more enzymes showed activity, although to very different extents. The three most active mutants, Gly87, Ala87 and Val87, and mutant Tyr87 all showed the highest activity with *n*-pentoxyresorufin as substrate; both increasing or decreasing the *n*-alkoxy-substituent leads to gradual decrease in activity. For the mutants with polar side chains, which show low *O*-dealkylation activity, generally the highest activity was found with the longer *n*-alkoxy-substituents (*n*-hexoxyresorufin to *n*-octoxyresorufin).

In addition to the *n*-alkoxy-substituted substrates, benzyloxyresorufin was used to characterize the different mutants. As shown in Table 3, benzyloxyresorufin is *O*-alkylated at relatively high activity by several mutants when compared to their activities toward the *n*-alkyoxyresorufins; for mutants Phe87, Leu87, Val87, Asn87, Gln87, Tyr87 and Arg87 the highest *O*-dealkylation was observed with this substrate. Similar to the *n*-alkoxy compounds, the highest activities were found in the mutants of small non-polar residues, with the highest activity in the case of mutants containing Val87, Gly87 and Ala87.

The different alkoxyresorufins were also incubated with wild-type BM3 containing a phenylalanine at position 87. Consistent with our previous study (*13*), wild-type BM3 showed no *O*-dealkylation activity with most alkoxyresorufins. Only with *n*-heptoxyresorufin and *n*-octoxyresorufine a low but significant resorufine production was found. To study whether long-chain alkoxyresorufins are hydroxylated at other positions of the *n*-alkoxy-chain, which would not result in *O*-dealkylation, incubations were analysed by UPLC with detection at 460 nm, which is absorption maximum of all alkoxyresorufins, independent of the nature of *n*-alkoxy-substituent. Chromatograms of these incubations measured at 460 nm, showed only strong peaks of the unchanged alkoxyresorufin substrates. Only extremely small peaks (less than 3% of parent compound) were found

[data not shown], indicating that side-chain hydroxylations did not occur to a significant extent.

2.3.2.2. NADPH-consumption and coupling efficiency

Table 4 shows the specific activities of the alkoxyresorufin-dependent NADPH consumption in incubations with BM3 M11 mutants and wild-type BM3.

The incubation conditions were similar to those of the fluorimetric *O*-dealkylation assays, except that the NADPH-regenerating system was excluded to enable NADPH-consumption to be measured. Surprisingly, all of the mutants tested showed a very high specific activity in NADPH-consumption. The highest activities were found in incubations with the mutant containing residue His87. This mutant showed specific activities higher than 6000 nmol NADPH/min/nmol P450, leading to complete consumption of NADPH within 4 minutes. The lowest activities were found in mutants containing residues Tyr87, Ile87, Leu87 and Met87.

Interestingly, for each mutant NADPH consumption was more or less similar for the substrates with the shorter *n*-alkoxy substituents, methoxyresorufin to *n*-pentoxyresorufin and allyloxyresorufin. For each mutant, the activities with these substrates varied by only 10 to 15%, which is close to the analytical error. These results suggest that for these alkoxyresorufins, NADPH-oxidation is not influenced by the length of the *n*-alkoxy-group. For substrates with longer *n*-alkoxy substituents, *n*-hexoxyresorufin to *n*-octoxyresorufin, NADPH oxidation gradually decreased with increasing *n*-alkoxy chain length. Also, in case of benzyloxyresorufin, having a bulky O-substituent, significantly lower NADPH-consumption was observed when compared to the other substrates.

Because no significant other metabolic pathways (side-chain hydroxylation) were found, the coupling efficiencies of the mutants were calculated from the ratio of the specific activities of resorufin production and NADPH-consumption (Table 5). Because of the very high rates of NADPH-consumption for all combinations of substrates and enzymes, extremely low coupling efficiencies were found. The highest coupling efficiencies were found with mutants containing Ala87 and Val87, with the highest coupling efficiencies of 0.68% (*n*-pentyl) and 0.75% (benzyl), respectively. For most reactions, the coupling efficiencies were too low to quantify because *O*-dealkylation activities were below the limit of detection. To test whether NADPH-consumption induced by alkoxyresorufin is the result of binding to the substrate binding site, it was tested whether 1 µM ketoconazole was able to block NADPH-consumption in incubations of wild-type BM3 and mutant Val87 (M11).

Table 3. Specific activities[a)] of alkoxyresorufin *O*-dealkylation by BM3 M11-mutants and wild-type BM3.

# Residue	Methyl (MROD)	Ethyl (EROD)	*n*-Propyl (PrROD)	*n*-Butyl (BuROD)	*n*-Pentyl (PROD)	*n*-Hexyl (HxROD)	*n*-Heptyl (HpROD)	*n*-Octyl (OROD)	Benzyl (BROD)
Non-polar side chain:									
1. Phe87	n.d. [c)]	n.d.	n.d.	n.d.	n.d.	0.11	0.16	0.060	0.29
2. Gly87	n.d.	n.d.	n.d.	1.01	3.80	2.59	0.74	0.14	4.02
3. Ala87	n.d.	0.16	1.53	4.37	11.05	1.83	0.34	0.10	3.79
4. Leu87	n.d.	n.d.	n.d.	n.d.	0.042	0.024	0.051	0.024	0.23
5. Ile87	n.d.	n.d.	n.d.	n.d.	0.35	0.010	0.062	n.d.	0.031
6. Val87 [b)]	n.d.	n.d.	0.75	1.08	1.64	0.42	0.11	0.068	5.43
7. Met87	n.d.	n.d.	n.d.	n.d.	n.d.	n.d.	n.d.	n.d.	n.d.
8. Pro87	-	-	-	-	-	-	-	-	-
9. Trp87	n.d.	n.d.	n.d.	n.d.	n.d.	n.d.	n.d.	n.d.	n.d.
Uncharged polar side chain:									
10. Ser87	-	-	-	-	-	-	-	-	-
11. Thr87	n.d.	n.d.	n.d.	0.12	n.d.	0.10	0.055	0.060	0.12
12. Asn87	n.d.	n.d.	n.d.	n.d.	n.d.	0.021	0.053	0.057	0.14
13. Gln87	n.d.	n.d.	n.d.	n.d.	n.d.	0.077	0.097	0.064	0.51
14. Tyr87	n.d.	0.024	0.13	0.14	0.55	0.076	0.017	0.031	0.92
15. Cys87	n.d.	n.d.	n.d.	n.d.	n.d.	0.026	n.d.	n.d.	n.d.
Charged polar side chain:									
16. Lys87	n.d.	n.d.	n.d.	n.d.	n.d.	n.d.	n.d.	n.d.	n.d.
17. Arg87	n.d.	n.d.	n.d.	n.d.	n.d.	0.013	0.010	0.028	0.038
18. His87	n.d.	n.d.	n.d.	n.d.	n.d.	0.046	0.022	0.046	n.d.
19. Asp87	-	-	-	-	-	-	-	-	-
20. Glu87	-	-	-	-	-	-	-	-	-
21. WT (Phe87) [d)]	n.d.	n.d.	n.d.	n.d.	n.d.	0.17	0.18	n.d.	n.d.

a) Specific activities (nmol resorufin/min/nmol P450) observed at 20 µM alkoxyresorufin and 20 nM of P450 BM3. Values represent averages of three measurements; standard deviations were less than 10%. b) Val87 = BM3 M11. c) n.d., not detectable (< 0.01 nmol/min/nmol P450). d) WT (Phe87), wild-type BM3.

Table 4. Specific activities [a] of alkoxyresorufin-induced NADPH-consumption by BM3 M11 mutants and wild-typeBM3

# Residue	Methyl (MROD)	Ethyl (EROD)	*n*-Propyl (PrROD)	*n*-Butyl (BuROD)	*n*-Pentyl (PROD)	*n*-Hexyl (HxROD)	*n*-Heptyl (HpROD)	*n*-Octyl (OROD)	Benzyl (BROD)	DMSO
Non-polar side chain:										
1. Phe87	4100	4590	3640	4520	4290	3120	1150	370	2170	< 10
2. Gly87	4380	3910	3950	4440	4170	2200	960	300	2360	105
3. Ala87	1860	1800	1510	1910	1620	550	300	130	950	90
4. Leu87	1180	1120	960	1110	540	260	270	190	190	95
5. Ile87	820	930	770	730	360	180	100	110	200	85
6. Val87 [b]	2930	2660	2590	3180	2100	900	290	310	720	190
7. Met87	1030	760	660	920	880	140	110	75	400	25
8. Pro87	-	-	-	-	-	-	-	-	-	-
9. Trp87	2090	1790	1450	1880	1980	870	320	130	1450	45
Uncharged polar side chain:										
10. Ser87	-	-	-	-	-	-	-	-	-	-
11. Thr87	1910	1570	1530	1900	1890	800	470	260	480	<10
12. Asn87	3260	2950	2450	2920	2970	1530	730	250	2260	<10
13. Gln87	1860	1740	1510	1770	1920	700	420	200	1130	40
14. Tyr87	700	680	620	710	690	400	130	87	370	<10
15. Cys87	3570	3490	3030	3430	3470	1590	560	150	2370	35
Charged polar side chain:										
16. Lys87	3570	3400	3080	4100	3780	1580	600	210	2220	<10
17. Arg87	3740	3780	2950	3400	2970	840	240	97	1330	25
18. His87	6110	6080	5650	5600	5600	2240	1650	890	5100	<10
19. Asp87	-	-	-	-	-	-	-	-	-	-
20. Glu87	-	-	-	-	-	-	-	-	-	-
21. WT (Phe87)	4650	3970	3290	4220	4020	2260	1030	730	4110	45

a) Specific activities (nmol resorufin/min/nmol P450). Values represent averages of three measurements; standard deviations were less than 10%. b) Val87 = BM3 M11. c) n.d., not detectable (< 0.01 nmol/min/nmol P450). d) WT (Phe87), wild-type BM3.

Table 5. Coupling efficiency (%)[a)] of alkoxyresorufin *O*-dealkylation by BM3 M11-mutants and wild-type BM3.

# Residue	Methyl (MROD)	Ethyl (EROD)	*n*-Propyl (PrROD)	*n*-Butyl (BuROD)	*n*-Pentyl (PROD)	*n*-Hexyl (HxROD)	*n*-Heptyl (HpROD)	*n*-Octyl (OROD)	Benzyl (BROD)
Non-polar side chain:									
1. Phe87	n.d. [b)]	n.d.	n.d.	n.d.	n.d.	0.004	0.014	0.016	0.013
2. Gly87	n.d.	n.d.	n.d.	0.023	0.091	0.118	0.077	0.047	0.170
3. Ala87	n.d.	n.d.	0.101	0.229	0.682	0.333	0.113	0.077	0.399
4. Leu87	n.d.	n.d.	n.d.	n.d.	0.008	0.009	0.019	0.013	0.121
5. Ile87	n.d.	n.d.	n.d.	n.d.	0.097	0.006	0.062	n.d.	0.016
6. Val87 [c)]	n.d.	n.d.	0.029	0.034	0.078	0.047	0.038	0.022	0.754
7. Met87	n.d.	n.d.	n.d.	n.d.	n.d.	n.d.	n.d.	n.d.	n.d.
8. Pro87	-	-	-	-	-	-	-	-	-
9. Trp87	n.d.	n.d.	n.d.	n.d.	n.d.	n.d.	n.d.	n.d.	n.d
Uncharged polar side chain:									
10. Ser87	-	-	-	-	-	-	-	-	-
11. Thr87	n.d.	n.d.	n.d.	0.006	n.d.	0.013	0.012	0.023	0.025
12. Asn87	n.d.	n.d.	n.d.	n.d.	n.d.	0.001	0.007	0.023	0.006
13. Gln87	n.d.	n.d.	n.d.	n.d.	n.d.	0.011	0.023	0.032	0.045
14. Tyr87	n.d.	0.004	0.021	0.020	0.080	0.019	0.013	0.036	0.249
15. Cys87	n.d.	n.d.	n.d.	n.d.	n.d.	0.002	n.d.	n.d.	n.d
Charged polar side chain:									
16. Lys87	n.d.	n.d.	n.d.	n.d.	n.d.	n.d.	n.d.	n.d.	n.d.
17. Arg87	n.d.	n.d.	n.d.	n.d.	n.d.	0.002	0.042	0.029	0.003
18. His87	n.d.	n.d.	n.d.	n.d.	n.d.	0.002	0.001	0.005	n.d
19. Asp87	-	-	-	-	-	-	-	-	-
20. Glu87	-	-	-	-	-	-	-	-	-
21. WT (Phe87) [d)]	n.d.	n.d.	n.d.	n.d.	n.d.	n.d.	0.016	0.025	n.d.

a) Coupling efficiencies were calculated by the formula: specific activity of resorufine production (Table 3) / specific activity of NADPH consumption (Table 4) x 100%. b) n.d., not detectable (< 0.001 %). c) Val87 = P450 BM3 M11. d) WT (Phe87), wild-type P450 BM3.

To test whether this concentration of ketoconazole was able to inhibit BM3, we first investigated whether it was able to block NADPH-consumption induced by 0.1 mM lauric acid. With both wild-type BM3 and mutant Val87, lauric acid strongly stimulated NADPH- consumption. Addition of 1 μM ketoconazole completely blocked lauric acid induced NADPH-consumption of both enzymes. When wild-type BM3 and mutant Val87 (M11) were tested with benzyloxyresorufine as substrate, ketoconazole was also able to almost completely block substrate-induced NADPH consumption as well as O-dealkylation reaction [data not shown].

2.3.2.3. Binding spectra.

Titration of alkoxyresorufins to solutions of BM3 and the two selected BM3 M11 mutants (Ala87 and Val87) in all cases resulted in typical type I difference spectra with a peak at 390 nm and a trough at 419 nm [data not shown], indicative of the conversion of the heme iron from low spin to high spin. Table 6 shows the dissociation constants (K_D) obtained by nonlinear fitting of the $\Delta A_{390-419}$ versus substrate concentration curves, after correction for dilution. Surprisingly, methoxyresorufin, which is not O-demethylated by any of the mutants, binds to the selected mutants with relatively high affinity with binding constants ranging from 2.4 to 8 μM (Table 6).

Table 6. Alkoxyresorufin binding by wild-type BM3 and BM3 M11-mutants.

	Methyl (MROD)	*n*-Butyl (BuROD)	*n*-Heptyl (HpROD)	Benzyl (BROD)
Substrate	K_D (μM) [a)]	K_D (μM) [a)]	K_D (μM) [a)]	K_D (μM) [a)]
wt BM3	8.4 ± 1.4	1.6 ± 0.2	22 ± 6.4	2.7 ± 0.4
BM3 M11 Ala87	4.0 ± 0.5	1.1 ± 0.1	4.9 ± 0.4	1.4 ± 0.3
BM3 M11 Val87	2.4 ± 0.2	0.8 ± 0.1	1.4 ± 0.2	1.8 ± 0.3

a) Dissociation constants were determined by difference spectroscopy using 2 μM enzyme in 100 mM potassium phosphate buffer, pH 7.4, titrated with a solution of substrate. All substrates produced a Type I binding spectrum with a peak at 390 nm and trough at 419 nm. The data for the absorbance at 419 nm minus the absorbance at 390 were corrected for dilution and fitted to an equation for a bimolecular association reaction to obtain the dissociation constant.

Because enzyme activity measurements were carried out with 20 μM substrate, it can be concluded that the lack of O-dealkylation is most likely due to nonproductive binding rather than lack of affinity for the enzyme. Wild-type BM3, which only showed very low O-dealkylation activity toward *n*-heptoxyresorufin, showed higher affinity for the other alkoxyresorufins which are not O-dealkylated. BM3 M11 mutants containing Ala87 and Val87, which generally showed relatively high O-dealkylation activity, showed slightly

higher affinity for the alkoxyresorufins than wild-type BM3. The only substrate showing significantly lower affinity for wild-type BM3 when compared with the BM3 mutants was *n*-heptoxyresorufin (Figure 1).

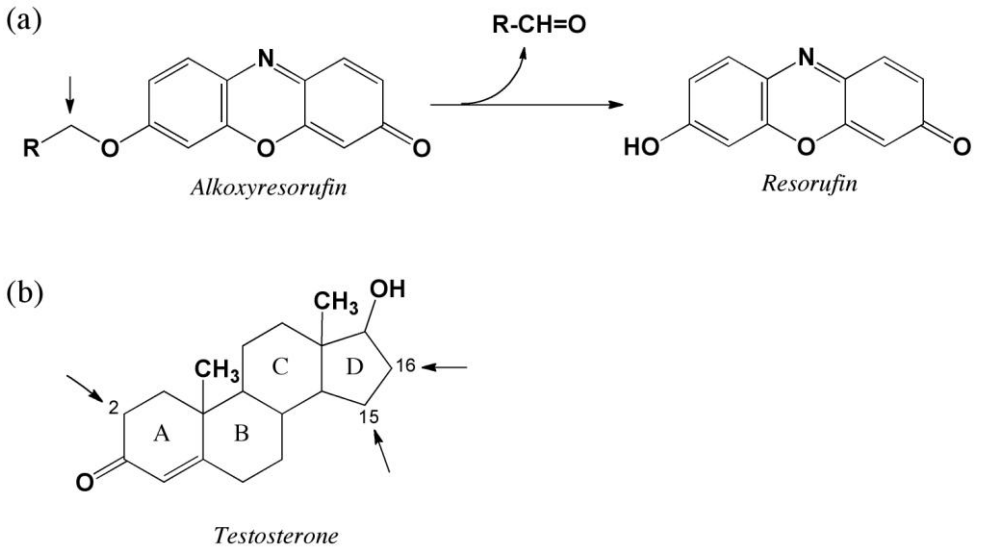

Figure 1. Structures and reactions of substrates used to characterize the BM3-mutants. (a) Alkoxyresorufine *O*-dealkylation: R = H (MROD), CH_2- (EROD), C_2H_4 (PrROD), C_3H_6 (BuROD), C_4H_8 (PROD), C_5H_{10} (HxROD), C_6H_{12} (HpROD), C_7H_{14} (OROD), CH_2=CH- (AllROD), phenyl (BROD). (b) Testosterone hydroxylation: arrows indicate identified positions of hydroxylation.

2.3.3. Testosterone hydroxylation by the BM3 M11-mutants.

Analysis of incubations of the BM3 mutants with testosterone by UPLC showed that three major metabolites were produced eluting at 0.93, 1.48 and 1.69 minutes. These metabolites corresponded to the three hydroxytestosterone metabolites previously observed with triple mutant BM3 R47L/F87V/L188Q (*26*). Figure 2 shows the chromatograms obtained after incubations of testosterone with mutants containing residues Tyr87, Ala87, Phe87 and Ile87, since they are representative of the diversity in the metabolic profiles obtained.

The metabolite eluted at 1.48 min was previously identified as 16β-hydroxytestosterone (16β-OH-T) (*26*). For structure elucidation of the other metabolites, large scale (50 mL) incubations were performed for 3 hours containing 250 nM of mutant Val87 (P450 M11),

500 µM testosterone, 0.2 mM NADPH and a regenerating system (0.3 mM glucose-6-phosphate and 0.4 U/mL glucose-6-phosphate dehydrogenase).

Metabolites were extracted by dichloromethane and isolated by preparative HPLC. Structure identification was performed by a combination of ^{1}D-^{1}H, ^{1}H-^{1}H-DQF-COSY, ^{1}H-^{13}C-HSQC, ^{1}H-^{13}C-HMQC, ^{1}H-^{13}C-HMBC and ^{1}H-^{1}H-NOESY NMR-experiments, which will be detailed in (*34*). The metabolite eluted at 0.93 min was identified as 15β-hydroxytestosterone (15β-OH-T), whereas the metabolite eluted at 1.69 min was identified as 2β-hydroxytestosterone (2β-OH-T). These two metabolites were previously also identified by similar NMR experiments as products formed in incubations of testosterone with housefly cytochrome P450 (CYP6A1) (*35*). Very minor metabolites were eluting at 1.85 and 1.95 minutes; however, the concentration of these metabolites was too low to allow structural assignment.

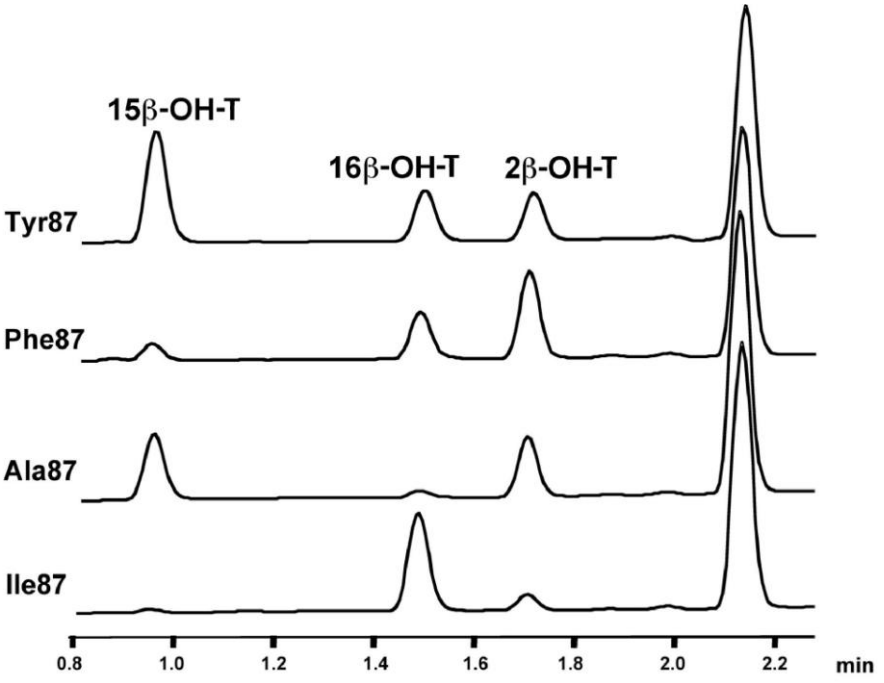

Figure 2. Ultraperformance liquid chromatography chromatograms obtained after incubations of testosterone (0.5 mM) with a selection of BM3 mutants (200 nM), representing the diversity in regioselectivity.

As shown in Table 7, all mutants were able to hydroxylate testosterone with widely different activities and with significant differences in metabolic profiles.

Table 7. Total activity and regioselectivity of testosterone hydroxylation by BM3 M11-mutants and wild-type BM3.

		Metabolite formation[a)]			
#	Residue	15β-OH-T	16β-OH-T	2β-OH-T	Total activity [a)]
Non-polar side chain					
1.	Phe87	86	275	499	860
2.	Gly87	31	13	12	56
3.	Ala87	356	25	244	625
4.	Leu87	2	9	35	46
5.	Ile87	21	597	92	710
6.	Val87 [b)]	641	351	218	1210
7.	Met87	11	33	36	81
8.	Pro87	-	-	-	-
9.	Trp87	15	6	8	29
Uncharged polar side chain					
10.	Ser87	-	-	-	-
11.	Thr87	126	367	557	1050
12.	Asn87	n.d.	n.d.	35	35
13.	Gln87	21	n.d.	119	140
14.	Tyr87	625	288	337	1250
15.	Cys87	1	n.d.	4	5
Charged polar side chain					
16.	Lys87	3	9	13	25
17.	Arg87	32	n.d.	33	65
18.	His87	40	n.d.	135	175
19.	Asp87	-	-	-	-
20.	Glu87	-	-	-	-
21.	WT (Phe87) [c)]	n.d.	n.d.	n.d.	n.d.

a) Specific activities (nmol hydroxytestosterone/nmol P450/60 minutes) observed at 0.5 mM testosterone and 200 nM of P450 BM3. Values represent averages of two measurements; variability was always less than 10%. b) BM3 M11. c) WT (Phe87), wild-type BM3. d) n.d., not detectable.

The most active mutants were Tyr87, Val87, Thr87, Phe87, Ile87 and Ala87 (in decreasing order); the other mutants showed activities less than 10% of that of Tyr87. In general, mutants having a very low activity with alkoxyresorufins as substrates also showed a low activity with testosterone as substrate, except for the mutants containing Phe87 and Thr87 which showed relatively high activity of testosterone hydroxylation. Incubation of wild-type BM3 did not show formation of any metabolites.

Figure 3 shows the metabolic profiles of the mutants ordered according to similarities in metabolic profiles, and by preference for hydroxylation of D-ring (e.g. 15ß-

and 16ß-hydroxylation) versus the A-ring (2ß-hydroxylation). Numbers below the bars represent the ratio of D-ring to A-ring hydroxylation, as calculated from the sum of peak areas of 15ß-OH-T and 16ß-OH-T, divided by the peak are of 2ß-OH-T.

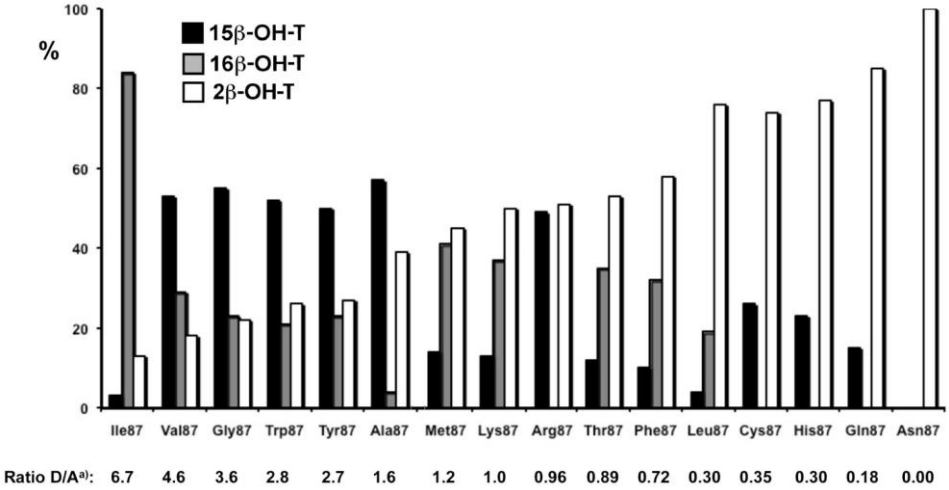

Figure 3. Effect of amino acid at position 87 on regioselective hydroxylation of testosterone by BM3 mutants. Bars represent percentage product relative to the total amount of products. Numbers below each bar represent the ratio of D-ring hydroxylation (sum of 15ß- and 16ß-hydroxylation) and A-ring hydroxylation (2ß-hydroxylation).

Mutants containing residues Ile87, Val87, Gly87, Tyr87, Trp87 and Ala87 all showed a preference for hydroxylation of the D-ring of testosterone. For mutants containing Val87, Gly87, Tyr87 and Trp87 very similar profiles were obtained with 15β-OH-T as major metabolite (50-55%), and with 16β-OH-T and 2β-OH-T formed in approximately equal amounts (20-25%). Compared to these mutants, the mutant containing Ala87 and Ile87 showed remarkable differences in regioselectivity of D-ring hydroxylation. The mutant containing Ile87 was the only mutant having high selectivity for 16ß-hydroxylation, whereas the mutant containing Ala87 showed predominantly 15ß-hydroxylation, in addition to significant 2ß-hydroxylation at the A-ring.

Mutants containing Phe87 and Thr87, which had relatively high activity, showed 2β-OH-T as major metabolite, with lower amounts of 16β-OH-T and the lowest amounts of 15β-OH-T. Similar results were obtained with the much less active mutants with residues Met87, Lys87 and Leu87. Mutants containing Cys87, His87, Gln87 and Asn87 also showed the highest preference of A-ring hydroxylation with 2β-OH-T as major metabolite. For three of these mutants D-ring hydroxylation was only found at the 15β-position; for Asn87 no significant D-ring hydroxylation was observed.

2.4.1 Discussion

The role of the residue at position 87 has been investigated in many studies using wild-type BM3 and mutants containing one or two other mutations, Table 1. These studies are hampered by the fact that only a limited number of substrates are accepted, such as medium-chain and long-chain fatty acids and small terpenoid and aromatic substrates. Also, so far only a limited number of amino acid substitutions have been evaluated at position 87. By far most studies have been performed with F87A and to a less extent with F87V and F87L. When applied to mutant 9-10A, containing R47C, V78A, K94I, P142S, T175I, A184V, F205C, S226R, H236Q, E252G, R255S, A290V and L353V, addition of mutation of F87A resulted in high enantioselectivity in buspirone hydroxylation (*16*), showing that residue 87 also has an important role in more promiscuous mutants of BM3. However, the effects of other amino acid substitutions were not reported.

In the present study, the role of position 87 in controlling substrate and regioselectivity of drug-metabolizing mutant BM3 M11 was evaluated, by creation of mutants with all twenty natural amino acids at this position. Twelve of the amino acid substitution had not yet been reported previously in any BM3 variant. To characterize the catalytic properties of these novel mutants, nine different alkoxyresorufins and testosterone were used as probe substrates.

As shown in Table 3 and 7, very significant different rates of product formation were found between the different mutants. In case of alkoxyresorufins as substrate, the mutant containing Phe87 only showed a very low *O*-dealkylation activity with longer-chain alkoxyresorufins starting from *n*-hexoxyresorufin, with activities similar to that obtained with wild-type BM3, which also contains Phe87. The mutants with the small non-polar amino acids Gly87, Ala87, Val87 and Ile87, all showed much higher *O*-dealkylation activities with an optimal activity with *n*-pentoxyresorufine as substrate (Table 3). As summarized in Table 1, replacement of the bulky Phe87 in wild-type BM3 by these small amino acids also showed generally an increased activity toward non-fatty acid substrates. Furthermore, the fact that mutants containing Val87, Leu87 and Ile87 showed large differences in activity towards *n*-alkoxyresorufins, and strongly different regioselectivity in testosterone hydroxylation, demonstrates that even minor changes in amino acid properties of the residue at position 87 can have a large effect on the catalyic properties.

It was proposed previously that replacement of the bulky Phe87 by smaller non-polar residues creates space for bulky substrates, allowing better positioning with respect to the activated oxygen species, and as a result higher activities and coupling efficiencies (*8, 10*). To test whether coupling efficiencies were affected by amino acid 87 substutions, the ratio of product formation to NADPH-consumption was studied. As shown in Table 4, extremely high activities of substrate-induced NADPH-consumption were found with all mutants and, unexpectedly, wild-type BM3. For the most active enzymes, the specific activities of NADPH-consumption were close to the high specific activities found with wild-type BM3 and lauric acid and arachidonic acid as substrates (*8, 9*). Because resorufin was

the only product found, the coupling efficiency was always less than 1% for all productive enzymes (Table 5). The fact that 20 µM of substrate resulted in complete depletion of 200 µM of NADPH within 2-3 minutes indicates that NADPH-consumption resulted from a catalytic process in which the substrate triggers NADPH-consumption without being converted, such as uncoupling, or redox-cycling in which the substrate undergoes one-electron reduction followed by autoxidation by molecular oxygen.

Uncoupling of P450 is still a poorly understood process, and it is considered to result from premature release of iron-bound molecular oxygen before completing the catalytic cycle, producing superoxide anion radical (one-electron reduction) or hydrogen peroxide (two-electron reduction; 'peroxide shunt') or by reduction of the $[FeO]^{3+}$ intermediate producing water (oxidase pathway) (*36, 37*). Factors which might determine the mode of uncoupling are active-site hydration, which might favor the peroxide shunt, and the position of the substrate in the active site and/or a large distance of the $[FeO]^{3+}$ intermediate to the substrate (*36, 37*). Because the mutants contain amino acids at position 87 with different polarities and size, different modes of uncoupling might underly the high NADPH-consumptions observed in the present study. An alternative mechanism which might explain alkoxyresorufin-induced NADPH-consumption is reduction of alkoxyresorufin at the level of the reductase domain. Previously it was shown that rat liver microsomal NADPH-cytochrome P450 reductase was able to catalyze redox-cycling of resorufin by one-electron reduction of the quinoneimine moiety (*38*). However, the fact that ketoconazole was able to almost completely inhibit alkoxyresorufin-induced NADPH-consumption by wild-type BM3 and mutant Val87, does not support this alternative mechanism. Also, the fact that alkoxyresorufins produce type I binding spectra when titrated to BM3 and BM3 mutants (Table 6) indicates that these substrates bind with relatively high affinity to the substrate binding site of these enzymes. These results strongly suggest that alkoxyresorufins bind to BM3 at the active site mainly in a nonproductive orientation. However, the mechanism by which alkoxyresorufine stimulated extremely high NADPH-consumption in these BM3 mutants and wild-type BM3 still remains to be elucidated.

Previously, several mutations of position 87 in wild-type BM3 were shown to change regioselectivity and stereoselectivity of several reactions, Table 1. In this study, testosterone was used as substrate to characterize the regioselectivity of the different mutants. It was found that all mutants tested were able to catalyze testosterone hydroxylation although at widely different activities and with different regioselectivities, Table 6. Only three different metabolites were formed at significant amount, as was shown previously in incubations with the triple-mutant of BM3, containing mutations R47L, F87V and L188Q (*26*). Interestingly, the mutant containing Phe87 appeared to be a relatively active enzyme, whereas the wild-type BM3 which also contains Phe87, was completely inactive.

Structural identification of the metabolites by NMR revealed that two of the metabolites result from hydroxylation of the D-ring, at positions 15ß and 16ß; the third metabolite results from hydroxylation of the A-ring at position 2ß. Available crystal structures of BM3 indicate that its substrate-binding site is a long hydrophobic channel, with the heme iron located at the bottom of this channel (*6*). This might explain why only the protons of the A-ring and D-ring of testosterone might approach the reactive iron-oxo species close enough to become hydroxylated.

As shown in Figure 3, several mutants have a strong preference for D-ring hydroxylation whereas others prefer hydroxylation at the A-ring. The mutant containing isoleucine at position 87 catalyzes predominantly 16ß-hydroxylation, whereas in case of the closely related leucine amino acid testosterone hydroxylation takes place predominantly as 2ß-hydroxylation. Why these relatively small change in amino acid side-chain have such a large effect on regioselectivity remains to be established however. Screening of over 200 microbial P450s (*27*) and genetic engineering of bacterial P450s previously enabled the identification of several other P450s that can catalyze 2ß- and 15ß-hydroxylation of testosterone (*27, 39*). Although several enzymes were shown to catalyze 16β–hydroxylation, so far no bacterial P450s have been reported that can catalyse 16ß-hydroxylation of steroids. The present study shows that the BM3 mutant containing Ile87 is the first mutant with high selectivity for 16ß-hydroxylation.

As summarized in Table 1, by far most amino acid substitutions at position 87 which have been reported involved mutations of Phe87 to amino acids with small non-polar side chains. Only two amino acids (Tyr and Ser) with uncharged polar side chains have been studied, whereas charged polar side chains have not been evaluated so far. Mutation F87Y, when applied to wild-type BM3, resulted in an unproductive enzyme when long-chain fatty acids were used as substrate (*8, 9, 17*).

The increased polarity caused by the hydroxyl-group at the phenyl-ring of Tyr87 was considered to restrict heme accessibility of the fatty acid substrates, and as a result causes full uncoupling (*8*). In the present study the mutant containing Tyr87 appeared more active than that containing Phe87 with both alkoxyresorufins and testosterone as substrate. Although Ser87 was not evaluated because carbon monoxide difference spectrum only showed P420 spectrum, the mutant containing Thr87 showed a P450 spectrum, and was one of the most active mutants with testosterone as substrate, Table 7. The other uncharged and charged polar amino acids also showed enzyme activity, although this was generally low when compared with the enzyme activity of the non-polar amino acids. However, the substrates used in the present study all concerned uncharged substrates. Therefore, it remains to be evaluated wheter the mutants containing the polar amino acids at position 87 will have higher affinity and activity with charged and polar substrates.

In conclusion, the results of the present study show that, consistent with the results of studies performed with wild-type enzyme, the nature of amino acid at position 87 has a strong effect on activity and regioselectivity of drug metabolizing mutants of BM3. Several amino acid substitutions not previously evaluated were shown to be, dependent on the substrate tested, active enzymes with different substrate- and regio-selectivity. Because of the wide substrate selectivity of BM3 M11 when compared to wild-type BM3, this panel of mutants will be useful as biocatalysts for metabolite production. Furthermore, these mutants might be valuable model proteins for mechanistic studies on the function of P450s in drug metabolism.

References

1. **Rankin, S. C., Aceto, H., Cassidy, J., Holt, J., Young, S., Love, B., Tewari, D., Munro, D. S., and Benson, C. E.** (2002) Molecular characterization of cephalosporin-resistant Salmonella enterica serotype Newport isolates from animals in Pennsylvania, *J Clin Microbiol 40*, 4679-4684.
2. **Warman, A. J., Roitel, O., Neeli, R., Girvan, H. M., Seward, H. E., Murray, S. A., McLean, K. J., Joyce, M. G., Toogood, H., Holt, R. A., Leys, D., Scrutton, N. S., and Munro, A. W.** (2005) Flavocytochrome P450 BM3: an update on structure and mechanism of a biotechnologically important enzyme, *Biochem Soc Trans 33*, 747-753.
3. **Eiben, S., Kaysser, L., Maurer, S., Kuhnel, K., Urlacher, V. B., and Schmid, R. D.** (2006) Preparative use of isolated CYP102 monooxygenases -- a critical appraisal, *J Biotechnol 124*, 662-669.
4. **Sawayama, A. M., Chen, M. M., Kulanthaivel, P., Kuo, M. S., Hemmerle, H., and Arnold, F. H.** (2009) A panel of cytochrome P450 BM3 variants to produce drug metabolites and diversify lead compounds, *Chemistry 15*, 11723-11729.
5. **van Vugt-Lussenburg, B. M., Stjernschantz, E., Lastdrager, J., Oostenbrink, C., Vermeulen, N. P., and Commandeur, J. N.** (2007) Identification of critical residues in novel drug metabolizing mutants of cytochrome P450 BM3 using random mutagenesis, *J Med Chem 50*, 455-461.
6. **Li, H., and Poulos, T. L.** (1997) The structure of the cytochrome p450BM-3 haem domain complexed with the fatty acid substrate, palmitoleic acid, *Nat Struct Biol 4*, 140-146.
7. **Oliver, C. F., Modi, S., Sutcliffe, M. J., Primrose, W. U., Lian, L. Y., and Roberts, G. C.** (1997) A single mutation in cytochrome P450 BM3 changes substrate orientation in a catalytic intermediate and the regiospecificity of hydroxylation, *Biochemistry 36*, 1567-1572.
8. **Graham-Lorence, S., Truan, G., Peterson, J. A., Falck, J. R., Wei, S., Helvig, C., and Capdevila, J. H.** (1997) An active site substitution, F87V, converts cytochrome P450 BM-3 into a regio- and stereoselective (14S,15R)-arachidonic acid epoxygenase, *J Biol Chem 272*, 1127-1135.
9. **Noble, M. A., Miles, C. S., Chapman, S. K., Lysek, D. A., MacKay, A. C., Reid, G. A., Hanzlik, R. P., and Munro, A. W.** (1999) Roles of key active-site residues in flavocytochrome P450 BM3, *Biochem J 339 (Pt 2)*, 371-379.
10. **Carmichael, A. B., and Wong, L. L.** (2001) Protein engineering of Bacillus megaterium CYP102. The oxidation of polycyclic aromatic hydrocarbons, *European journal of biochemistry / FEBS 268*, 3117-3125.
11. **Li, Q. S., Ogawa, J., Schmid, R. D., and Shimizu, S.** (2001) Residue size at position 87 of cytochrome P450 BM-3 determines its stereoselectivity in propylbenzene and 3-chlorostyrene oxidation, *FEBS letters 508*, 249-252.
12. **Li, Q. S., Ogawa, J., Schmid, R. D., and Shimizu, S.** (2001) Engineering cytochrome P450 BM-3 for oxidation of polycyclic aromatic hydrocarbons, *Applied and environmental microbiology 67*, 5735-5739.
13. **Lussenburg, B. M., Babel, L. C., Vermeulen, N. P., and Commandeur, J. N.** (2005) Evaluation of alkoxyresorufins as fluorescent substrates for cytochrome P450 BM3 and site-directed mutants, *Analytical biochemistry 341*, 148-155.

14. **Sowden, R. J., Yasmin, S., Rees, N. H., Bell, S. G., and Wong, L. L.** (2005) Biotransformation of the sesquiterpene (+)-valencene by cytochrome P450cam and P450BM-3, *Organic & biomolecular chemistry 3*, 57-64.
15. **Sulistyaningdyah, W. T., Ogawa, J., Li, Q. S., Maeda, C., Yano, Y., Schmid, R. D., and Shimizu, S.** (2005) Hydroxylation activity of P450 BM-3 mutant F87V towards aromatic compounds and its application to the synthesis of hydroquinone derivatives from phenolic compounds, *Applied microbiology and biotechnology 67*, 556-562.
16. **Landwehr, M., Hochrein, L., Otey, C. R., Kasrayan, A., Backvall, J. E., and Arnold, F. H.** (2006) Enantioselective alpha-hydroxylation of 2-arylacetic acid derivatives and buspirone catalyzed by engineered cytochrome P450 BM-3, *Journal of the American Chemical Society 128*, 6058-6059.
17. **Kitazume, T., Haines, D. C., Estabrook, R. W., Chen, B., and Peterson, J. A.** (2007) Obligatory intermolecular electron-transfer from FAD to FMN in dimeric P450BM-3, *Biochemistry 46*, 11892-11901.
18. **Chen, C. K., Shokhireva, T., Berry, R. E., Zhang, H., and Walker, F. A.** (2008) The effect of mutation of F87 on the properties of CYP102A1-CYP4C7 chimeras: altered regiospecificity and substrate selectivity, *Journal of biological inorganic chemistry : JBIC : a publication of the Society of Biological Inorganic Chemistry 13*, 813-824.
19. **Dietrich, M., Do, T. A., Schmid, R. D., Pleiss, J., and Urlacher, V. B.** (2009) Altering the regioselectivity of the subterminal fatty acid hydroxylase P450 BM-3 towards gamma- and delta-positions, *Journal of biotechnology 139*, 115-117.
20. **Kim, D. H., Ahn, T., Jung, H. C., Pan, J. G., and Yun, C. H.** (2009) Generation of the human metabolite piceatannol from the anticancer-preventive agent resveratrol by bacterial cytochrome P450 BM3, *Drug metabolism and disposition: the biological fate of chemicals 37*, 932-936.
21. **Seifert, A., Vomund, S., Grohmann, K., Kriening, S., Urlacher, V. B., Laschat, S., and Pleiss, J.** (2009) Rational design of a minimal and highly enriched CYP102A1 mutant library with improved regio-, stereo- and chemoselectivity, *Chembiochem : a European journal of chemical biology 10*, 853-861.
22. **Damsten, M. C., van Vugt-Lussenburg, B. M., Zeldenthuis, T., de Vlieger, J. S., Commandeur, J. N., and Vermeulen, N. P.** (2008) Application of drug metabolising mutants of cytochrome P450 BM3 (CYP102A1) as biocatalysts for the generation of reactive metabolites, *Chemico-biological interactions 171*, 96-107.
23. **Burke, M. D., Thompson, S., Weaver, R.J., Wolf, C.R. and Mayer, R.T.** (1994) Cytochrome P450 specificities of alkoxyresorufin O-dealkylation in human and rat liver, *Biochem. Pharmacol. 48*, 923-936.
24. **Burke, M. D., and Mayer, R. T.** (1983) Differential effects of phenobarbitone and 3-methylcholanthrene induction on the hepatic microsomal metabolism and cytochrome P-450-binding of phenoxazone and a homologous series of its n-alkyl ethers (alkoxyresorufins), *Chemico-biological interactions 45*, 243-258.
25. **Burke, M. D., Thompson, S., Elcombe, C.R., Halpert, J., Haaparanta, T., Mayer, R.T.** (1983) Ethoxy-, pentoxy- and benzyloxyphenoxazones and homologues: a

series of substrates to distinguish between different induced cytochromes P450, *Biochem Pharmacol 34*, 3337-3345.

26. **van Vugt-Lussenburg, B. M., Damsten, M. C., Maasdijk, D. M., Vermeulen, N. P., and Commandeur, J. N.** (2006) Heterotropic and homotropic cooperativity by a drug-metabolising mutant of cytochrome P450 BM3, *Biochem Biophys Res Commun 346*, 810-818.
27. de Vlieger, J. S., Kolkman, A. J., Ampt, K. A., Commandeur, J. N., Vermeulen, N. P., Kool, J., Wijmenga, S. S., Niessen, W. M., Irth, H., and Honing, M. (2010) Determination and identification of estrogenic compounds generated with biosynthetic enzymes using hyphenated screening assays, high resolution mass spectrometry and off-line NMR, *Journal of chromatography. B, Analytical technologies in the biomedical and life sciences 878*, 667-674.
28. **Agematu, H., Matsumoto, N., Fujii, Y., Kabumoto, H., Doi, S., Machida, K., Ishikawa, J., and Arisawa, A.** (2006) Hydroxylation of testosterone by bacterial cytochromes P450 using the Escherichia coli expression system, *Bioscience, biotechnology, and biochemistry 70*, 307-311.
29. **Fernandes, P., Cruz, A., Angelova, B., Pinheiro, H.M., Cabral, J.M.S.** (2003) Microbial conversion of steroid compounds: recent developments, *Bioscience, biotechnology, and biochemistry 70*, 307-311.
30. **Omura, T., and Sato, R.** (1964) The Carbon Monoxide-Binding Pigment of Liver Microsomes. Ii. Solubilization, Purification, and Properties, *The Journal of biological chemistry 239*, 2379-2385.
31. **Wang, D., and Zhang, M.** (2007) Rapid quantitation of testosterone hydroxyl metabolites by ultra-performance liquid chromatography and mass spectrometry, *Journal of chromatography. B, Analytical technologies in the biomedical and life sciences 855*, 290-294.
32. **Reinen, J., Ferman, S., Vottero, E., Vermeulen, N. P., and Commandeur, J. N.** (2011) Application of a fluorescence-based continuous-flow bioassay to screen for diversity of cytochrome P450 BM3 mutant libraries, *Journal of biomolecular screening 16*, 239-250.
33. **Perera, R., Sono, M., Sigman, J. A., Pfister, T. D., Lu, Y., and Dawson, J. H.** (2003) Neutral thiol as a proximal ligand to ferrous heme iron: implications for heme proteins that lose cysteine thiolate ligation on reduction, *Proceedings of the National Academy of Sciences of the United States of America 100*, 3641-3646.
34. **Rea, V., Kolkman, A. J., Vottero, E., Stronks, E. J., Ampt, K. A., Honing, M., Vermeulen, N. P., Wijmenga, S. S., and Commandeur, J. N.** (2012) Active site substitution A82W improves the regioselectivity of steroid hydroxylation by cytochrome P450 BM3 mutants as rationalized by spin relaxation nuclear magnetic resonance studies, *Biochemistry 51*, 750-760.
35. **Jacobsen, N. E., Kover, K. E., Murataliev, M. B., Feyereisen, R., and Walker, F. A.** (2006) Structure and stereochemistry of products of hydroxylation of human steroid hormones by a housefly cytochrome P450 (CYP6A1), *Magnetic resonance in chemistry : MRC 44*, 467-474.
36. **Loida, P. J., and Sligar, S. G.** (1993) Molecular recognition in cytochrome P-450: mechanism for the control of uncoupling reactions, *Biochemistry 32*, 11530-11538.

37. **Yeom, H., and Sligar, S. G.** (1997) Oxygen activation by cytochrome P450BM-3: effects of mutating an active site acidic residue, *Archives of biochemistry and biophysics 337*, 209-216.
38. **Dutton, D. R., Reed, G. A., and Parkinson, A.** (1989) Redox cycling of resorufin catalyzed by rat liver microsomal NADPH-cytochrome P450 reductase, *Archives of biochemistry and biophysics 268*, 605-616.
39. **Virus, C., Lisurek, M., Simgen, B., Hannemann, F., and Bernhardt, R.** (2006) Function and engineering of the 15beta-hydroxylase CYP106A2, *Biochemical Society transactions 34*, 1215-1218.